ISSN 2616-5767 Vol.6, Issue 12: 128-135, DOI: 10.25236/AJETS.2023.061219

Mechanical response of geocell reinforced wind-logged sand based on model test

Yuqin Zhang[1,a,*], Chang Liu[1]

[1]*Lanzhou Jiaotong University, Lanzhou, China*
[a]*chin.1997@foxmail.com*
[*]*Corresponding author*

Abstract: *Through The study investigated the impact of geocell reinforcement position and the number of reinforced layers on the bearing capacity and deformation characteristics of sandy embankments under various working conditions, through model tests of sandy embankments and geocell-reinforced sandy embankments. The study examined the impact of the position of geocell reinforcement and the number of reinforcement layers on the bearing capacity and deformation characteristics of windlogged sand embankments under various operational conditions. Additionally, it comparatively analyzed the soil pressure on the upper and lower sides of the geocell reinforcement position. The test results indicate that the use of geocell reinforcement in embankments can enhance the embankment's load-bearing capacity, mitigate uneven settlement and lateral deformation, and increase the ultimate bearing capacity by 83.3% when compared to a plain sand embankment under a three-layer reinforced condition. Furthermore, the geocell-reinforced layer can create a composite structure with the soil, distribute upper stress, expand the internal stress area of the embankment, and act as a frictional constraint to limit horizontal and vertical soil deformation, reduce settlement, and enhance the damage mechanism of both the embankment and the reinforced embankment. Decreasing the settlement enhances the bearing capacity and stability of the embankment.*

Keywords: *Reinforced Embankment; Windlogged Sand; Geocells; Modelling Tests; Slope Stability*

1. Introduction

Geocell, a frequently utilized reinforcement material, enhances the lateral restraining effect on the soil body in comparison to other traditional reinforcing materials, owing to its three-dimensional mesh structure[1]. It is commonly employed to reinforce non-cohesive bulk sandy soil roadbeds in routine construction practices, leading to a notable enhancement in the bearing capacity and stability of wind-logged sandy embankments, as well as the limitation of embankment deformation. As a result, geocells have found extensive application in diverse areas of transportation engineering.

Wang Yankun[2] conducted an analysis on the impact of geocell reinforcement by examining the stress-strain characteristics of geocell-reinforced wind-logged sand and the shear strength. The study demonstrated that geocell-reinforced wind-logged sand embankment can enhance the strength of wind-logged sand by 1.37 to 1.82 times. In a similar vein, Bindraratna[3] conducted a series of experiments to investigate the physico-mechanical properties of the reinforced roadbase under high-frequency cyclic triaxial tests. The research aimed to assess the influence of perimeter and bias stresses on the deformation (permanent and elastic) and degradation of the specimens. The test results indicate that there is an optimal range of circumferential pressures for minimizing the deformation of the specimens for each deviatoric stress set in the test. Sun Zhou[4] conducted model tests on both pure sand embankment slopes and geocell-reinforced embankments. The results indicated that the reinforcing effect improves with a smaller depth of the cell arrangement and welding distance, a larger number of layers, and higher degree of embankment soil compaction. The optimal conditions of the reinforced embankment led to a 1.5 times increase in bearing capacity. Similarly, Wang Xuancang[5] performed centrifugal model tests on geocell-reinforced roadbeds, demonstrating that the cell reinforcement reduces roadbed settlement. Specifically, settlement under two-layer and three-layer reinforcement conditions decreased by 32% compared to plain soil roadbeds. Furthermore, Wang Qiang[6] investigated the friction characteristics of the reinforced-soil interface through indoor experiments and numerical simulations.

The study revealed that soil compaction and water content significantly influence friction behavior. The content has a greater impact on the reinforced-soil interfacial drag coefficient. As compaction

ISSN 2616-5767 Vol.6, Issue 12: 128-135, DOI: 10.25236/AJETS.2023.061219

increases or water content decreases, the interfacial drag coefficient also increases. The research showed that the compaction level and moisture content of the soil have a significant impact on the interfacial resistance coefficient of reinforced soil. Furthermore, the interfacial resistance coefficient increases as the compaction level increases or the water content decreases.

2. Model Test Study

2.1 Test Materials

2.1.1 Geocell

The geocell used in this test is made of non-porous PET sheet. The longitudinal tensile strength of the strip is ≥ 100 MPa in the cutting and punching. It is riveted through the angle coder to achieve the required test welding distance and the height of the chamber. The connection point has a tensile strength of ≥ 140 MPa, as shown in Fig. 1. The height of the chamber used in the test is 50 mm, and the welding distance is 150 mm.

Figure 1: Schematic Diagram of Geocell.

Table 1: Physical Characteristics.

Unevenness Coefficient Cu	2.66~3.25
Curvature Factor Cc	0.89~1.01
Moisture Content w/%	14
Maximum Dry Density ρdmax/g/cm3	1.83

2.1.2 Wind-logged Sand

After conducting an indoor geotechnical test on the wind-logged sand, the physical properties of the sand used in the test are presented in Table 1.

2.2 Test Setup

2.2.1 Model Box Arrangement

This test simulates the surface deformation of a reinforced sandy embankment under static load. It utilizes a self-made model box measuring 2.4m (L) × 1.2m (W) × 1.2m (H), which is reinforced with channel steel. The model box is depicted in Fig. 2.

2.2.2 Test Device

The indoor model test involves using jacks to apply a maximum displacement of 150mm and a maximum axial force of 20kN. The vertical load is measured using a counterforce frame and a pressure sensor on top of the jacks. The counterforce frame applies pressure to the top of the embankment using a loading plate with dimensions of 115mm × 25mm. The test includes tendons and instrumentation layout as depicted in Fig. 3.

ISSN 2616-5767 Vol.6, Issue 12: 128-135, DOI: 10.25236/AJETS.2023.061219

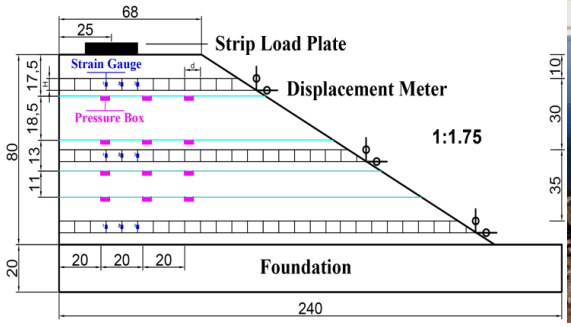

Figure 2: Model Box.

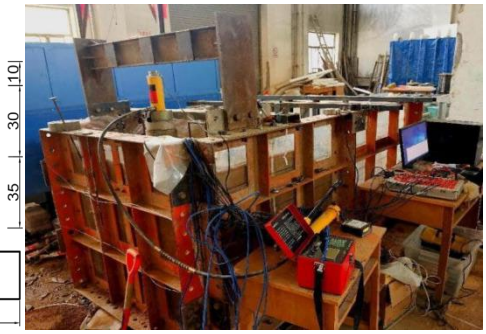

Figure 3: Layout Schematic.

2.3 Test Steps

This paper primarily divides the model test steps into layered compaction of fill sand, buried tendon material, instrumentation, loading, and data reading. Through manual compaction and the use of an electric tamping machine, the soil is compacted in layers to fill the embankment to reach the required compaction level, fill sand to the required height, and shape the cutting slopes to achieve the required gradient for the model.

According to the specification test, the failure criterion is met when there is significant extrusion of the soil outside the loading plate range, resulting in rapid settlement at the top of the slope, and continued slope displacement after the load is applied until reaching the peak. However, the bearing capacity cannot be increased, and it is considered that the embankment model will fail.

2.4 Test Programme

The model is used to investigate the impact of geocell-reinforced, wind-logged sand embankments on the bearing capacity and deformation characteristics of the embankment under various working conditions (reinforcement position and number of layers). To investigate the mechanism by which geocells enhance the bearing capacity of embankments and mitigate slope deformation and embankment damage, a 1:1.75 sandy embankment model with a 1:10 scale to the actual embankment was utilized in the test. The loading plate's center line was positioned 430mm from the top of the slope. The model box was filled with the ideal moisture content for conducting indoor model test research. The test was conducted with five different working conditions, as illustrated in Table 2. The compaction degree of the embankment was 90%. Working conditions 2 and 3 were utilized to compare the impact of the depth of reinforcement on the reinforcement effect, while working conditions 2, 4, and 5 were employed to assess the influence of the number of layers of reinforcement on the reinforcement effect.

Table 2: Test Conditions.

Working Condition	Typology	Position	Storey
1	Plain Soil		
2	Geocell	Upper Section	1
3	Geocell	Central Section	1
4	Geocell	Upper and Central Section	2
5	Geocell	Upper, Central and Lower Section	3

3. Test Results and Analysis

3.1 Comparative Analysis of p-s Settlement Curve and Ultimate Bearing Capacity

The maximum settlement of the strengthened embankment was recorded at -43.78mm, -39.92mm, -35.82mm, -31.78mm, and -29.41mm under varying operational circumstances, respectively. The settlement curves of the reinforced embankment model under various working conditions were generated using 20kPa incremental loading and the data from the slope top percentile table, as depicted in Figure 4. The curvature of the curve diminishes as the load increases, resulting in an increase in settlement at the top of the embankment slope. Once the ultimate load is reached, the settlement at the top of the slope increases rapidly. The inflection point of the settlement curve occurs at the ultimate load, leading to the

ISSN 2616-5767 Vol.6, Issue 12: 128-135, DOI: 10.25236/AJETS.2023.061219

structural destruction of the embankment and subsequent destabilization of the embankment model. Following the reinforcement of the embankment with geogrids, the geogrids function as mesh pockets, limiting soil displacement in the upper part of the reinforcement and enhancing the stability of the embankment. Following the implementation of a geocell-reinforced embankment, the geocell functions as a mesh pocket, constraining the displacement of the upper portion of the reinforcement and thereby enhancing the ultimate bearing capacity of the embankment.

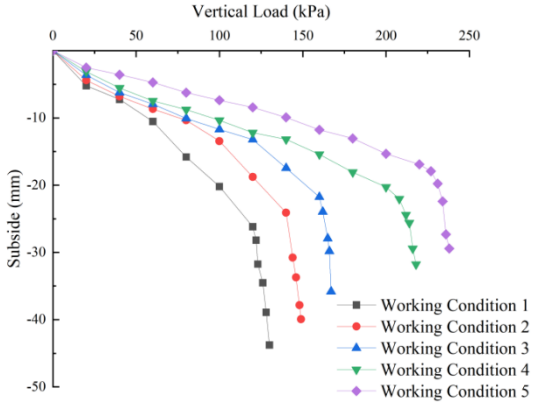

Figure 4: Modelling p-s Settlement Curves.

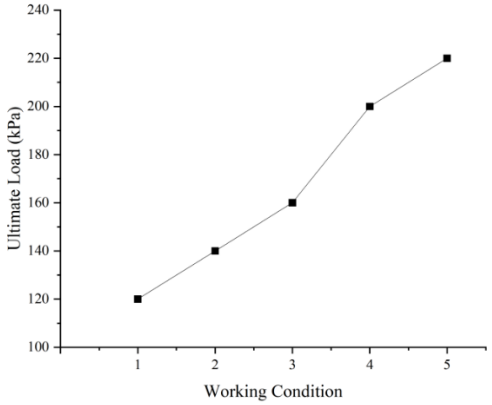

Figure 5: Modelling Ultimate Load.

Figures 4 and 5 analyze the settlement curve and ultimate bearing capacity of the reinforced embankment model in plain sand and with four types of reinforcement. The results indicate varying degrees of increase in the ultimate bearing capacity of the embankment after reinforcement, with inflection points observed in the ultimate bearing capacity curve. In comparison to the plain soil subgrade, the central single layer of reinforcement demonstrates a more significant improvement in bearing capacity, with increases of 33.3% and 16.7% for the central and upper reinforcement, respectively. Additionally, the two-layer reinforcement shows a 66.7% increase compared to plain sand, while the three-layer reinforcement exhibits an 83.3% increase.Compared to plain sand, the ultimate bearing capacity increases with the deepening of the lattice compartment and the increase of the number of layers in two-layer reinforcement by 66.7% and three-layer reinforcement by 83.3%. The stronger the constraints on reinforced embankment denaturation, the stronger the constraints on reinforced embankment denaturation. However, the depth of the reinforcement plays a positive role in the bearing capacity within a specific range of effect. If the reinforcement is buried too deep, the soil body will be damaged due to the absence of transmission of the reinforcement, resulting in the reinforcement not playing the role of frictional lateral limit. This leads to the restriction of lateral deformation of the soil body and the slope surface, causing damage to the embankment.

The settlement difference at the top of the slope is not significant in the initial two loading stages, as indicated by the curve. This can be attributed to the soil still being in the compaction stage under the load. Additionally, during the early loading stage, the upper tendon material restrains the soil body, while the loading plate continues to sink, transmitting the loading effect to the lower tendon material, which only begins to play a role at that point. Upon the placement of two layers of lattice room pavement, an increase in the ultimate load carrying capacity is observed alongside the settlement of the top of the slope. It is evident that during the destruction stage of settlement, the soil body does not exhibit the friction lateral limit of action, leading to embankment damage.The deceleration of settlement plate sinking during the destructive stage is attributed to the lateral frictional constraint exerted by the middle chamber, which restricts rapid soil displacement and mitigates the potential for sudden landslides.

3.2 Comparative Analysis of Slope Displacement of Reinforced Embankment

The histograms depicting the changes in measurement points under various working conditions were plotted by positioning the horizontal and vertical percentile meters at the top, middle, and foot of the embankment. This was achieved by reading the values during the loading process step by step, as illustrated in Figures 6 and 7.The horizontal displacement at the crest of the slope increases to 11.21mm upon reaching the ultimate load of 120kPa in the unreinforced sand embankment. The upper and middle single-layer reinforcements exhibit reductions of 12.04% and 17.03% respectively compared to the unreinforced sand. Furthermore, the two-layer and three-layer reinforcements experience reductions of 24.26% and 29.17% respectively. The horizontal displacement trends in the mid-slope and crest chamber constraints mirror those at the crest. Additionally, the two-layer and three-layer reinforcements

ISSN 2616-5767 Vol.6, Issue 12: 128-135, DOI: 10.25236/AJETS.2023.061219

demonstrate reductions of 24.26% and 29.17% respectively compared to the single-layer reinforcement. The impact of restraining displacement in the middle and top of the slope is similar when compared to single-layer reinforcement. This similarity can be attributed to the predominant occurrence of lateral deformation in the shallow area of the roadbed under load, with the lower and middle compartments playing a minor role in lateral restriction.

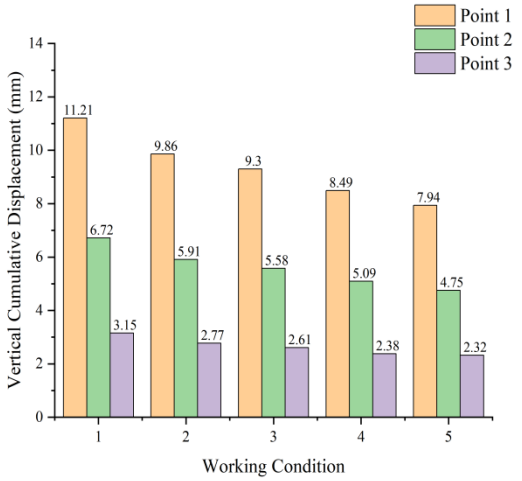

Figure 6: Modelling Vertical Displacement.

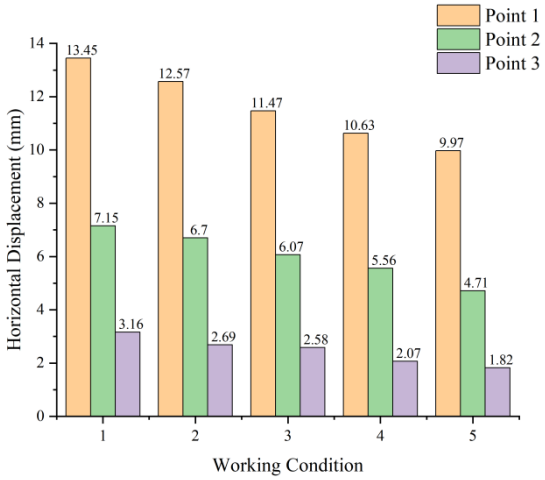

Figure 7: Modelling Horizontal Displacement.

3.3 Comparative Analysis of Soil Pressure inside Reinforced Embankments

In order to investigate the distribution pattern of additional earth pressure within the embankment, a total of 12 earth pressure boxes are positioned inside the embankment. Among these, T-1 to T-6 and T-10 to T-12 are utilized to monitor the additional stress within the embankment. The earth pressure distribution diagrams within the embankment under the four conditions are depicted in Fig. 8. It is observed that the earth pressure boxes T-1, T-4, and T-10 in the same longitudinal section for the plain soil embankment and the reinforced embankment exhibit a decrease with the increase in burial depth. The maximum additional soil pressure on the same horizontal plane decreases gradually in the direction away from the slope. After the grid chamber is laid, the maximum additional soil pressure at the same measurement point of the embankment model decreases to a different extent than that of the plain soil roadbed. The plain soil reinforcement demonstrates that the soil pressure at the measurement point beneath the load plate continues to increase even after reaching the ultimate load. However, in close proximity to the side slope, the T-4 pressure box begins to decrease, suggesting that the soil body in this area and the onset of instability have experienced compromised integrity.

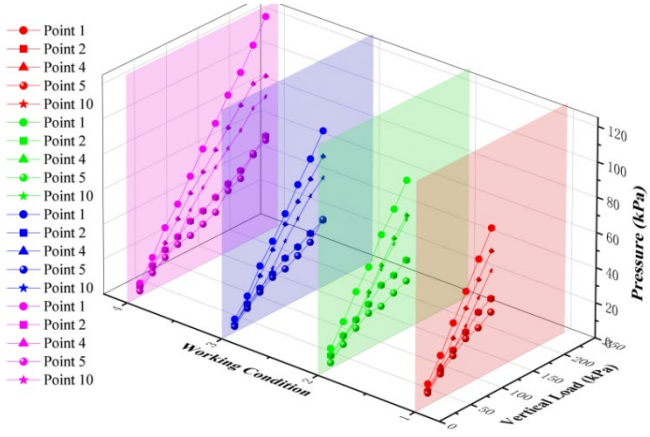

Figure 8: Soil pressure distribution diagram.

3.4 Comparative Analysis of Soil Pressure on the Upper and Lower Sides of the Geocell Reinforcement Position

The earth pressure boxes T-7, T-8, and T-9 were arranged on the lower side of the central reinforced position to compare and analyze the additional earth pressure on the upper and lower side of the

ISSN 2616-5767 Vol.6, Issue 12: 128-135, DOI: 10.25236/AJETS.2023.061219

reinforcement. The earth pressure on the upper and lower sides of the reinforcement under the two conditions are illustrated in Fig. 9 and Fig. 10. Under the condition of a single layer of reinforcement at the central part of the structure, the earth pressure on the upper and lower sides is reduced by 8.72%, 8.12%, and 7.67%, respectively, due to the reinforcement. This reduction increases to 9.17%, 8.93%, and 8.36%, respectively, when two layers of reinforcement are present. The earth pressure was reduced by 9.17%, 8.93%, and 8.36% in two layers of reinforced condition.

The geogrid arrangement layer appears to reduce the maximum additional stress to a certain extent. Additionally, as the additional earth pressure increases at the measurement point directly under the loading plate, there is a close correspondence between the increase in the value of the additional earth pressure near the direction of the slope and the gradual increase in the value of the additional earth pressure. This suggests a tendency for the earth pressure to become more uniform within the same layer after the reinforcement layer. Consequently, the stresses borne at the top of the embankment are dispersed, contributing to increased stability of the road. It is evident that following the addition of the reinforced layer, the soil pressure within the same layer tends to become more uniform. The stress at the crest of the embankment is distributed, allowing a broader section of the embankment to bear the load.

The geocell functions to diffuse stress, thereby decreasing stress concentration within the embankment and consequently enhancing the load-bearing capacity of the wind-affected sand embankment. Text: The analysis of the test results indicates that the central reinforcement demonstrates a more pronounced effect than the upper reinforcement stress diffusion. The reinforcement effect of two and three layers is particularly notable. Additionally, as the number of layers increases, the additional soil pressure at the same point decreases. This suggests that increasing the number of reinforcement layers can enhance the geocell stress diffusion. However, compared to two layers of reinforcement, the primary function of three layers is to prevent stress concentration at the base and facilitate stress diffusion. The geocell exhibits stress diffusion in the middle and upper parts of the embankment, thereby reducing stress concentration. In contrast to the use of two layers of reinforcement, the primary purpose of employing three layers of reinforcement is to mitigate stress concentration at the base and facilitate stress diffusion. However, the effectiveness of this approach in enhancing the middle and upper sections of the embankment is not readily apparent.

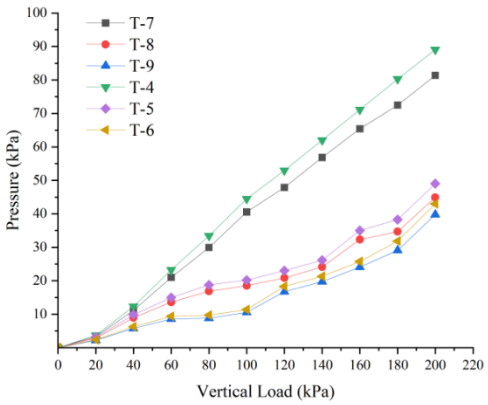

Figure 9: Comparison of Soil Pressure (a).

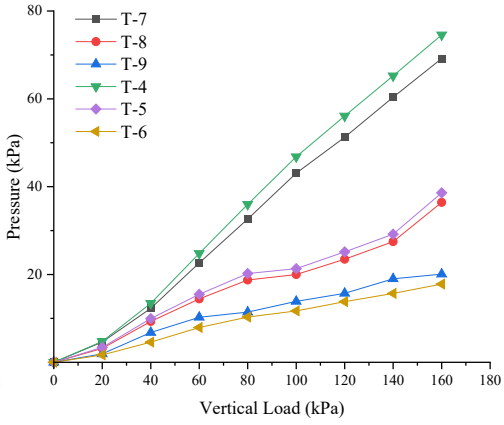

Figure 10: Comparison of Soil Pressure (b).

3.5 Comparative Stress-strain Analysis of Eeinforced Embankment Geocells

In the box in the tendon arrangement layer from the loading plate center to the slope direction to select three compartments to paste strain gauges, drawing vertical load and compartment tensile strain relationship curves in Fig. 11 and Fig. 12, it can be seen that the compartment tensile strain with the embankment at the top of the load and increase, when the load reaches 40kPa, when the compartment tensile strain When the load reaches 40kPa, when the compartment tensile strain increases, it produces lateral friction effect on the soil, the compartment tensile strain decreases gradually from the loading plate to the side slope, and the compartment is not damaged, only the bottom area of the loading plate produces bending deformation of the compartment downwards.

The high tensile strength of the compartment itself primarily restricts the full utilization of the material's tensile strength in the three layers of reinforcement under the loading plate. This results in the upper compartment reaching a maximum tensile strain of 0.282%. As the load increases, the growth amplitude of the compartment's tensile strain tends to moderate. This is attributed to the counteracting

ISSN 2616-5767 Vol.6, Issue 12: 128-135, DOI: 10.25236/AJETS.2023.061219

effect of the load's tensile stress on the compartment, which limits the horizontal deformation of the soil body and enhances the embankment's integrity.

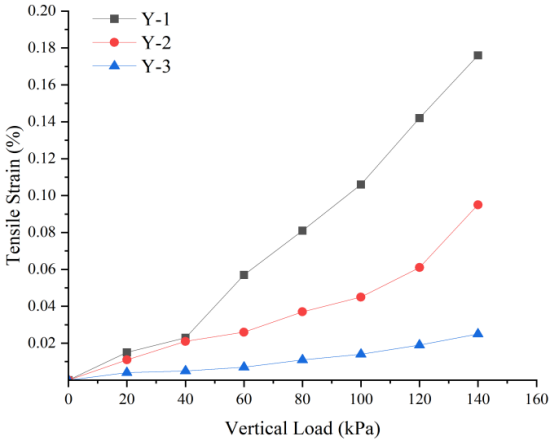

Figure 11: Geocell Strain (a).

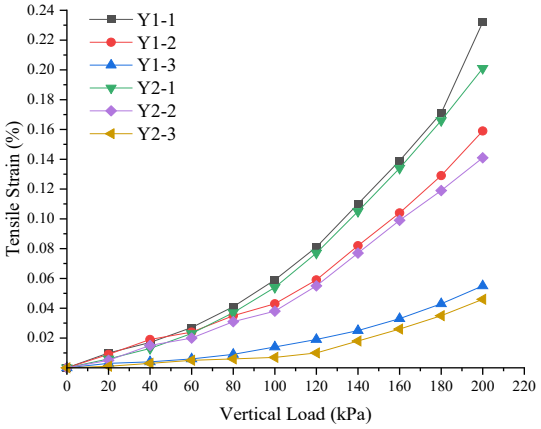

Figure 12: Geocell Strain (b).

3.6 Comparative Analysis of Damage Patterns on Reinforced Embankment Slopes

The forms of damage to reinforced embankments vary under different working conditions. Schematic diagrams were created based on the actual morphology of the embankment damage surface, as depicted in Figure 13. In the model of the plain soil embankment and the single-layer reinforced embankment, it is observed that the settlement at the crest of the slope exceeds the horizontal displacement of the slope. This indicates that the failure of the embankment structure is attributed to the destabilization of the foundation caused by excessive vertical displacement of the embankment.

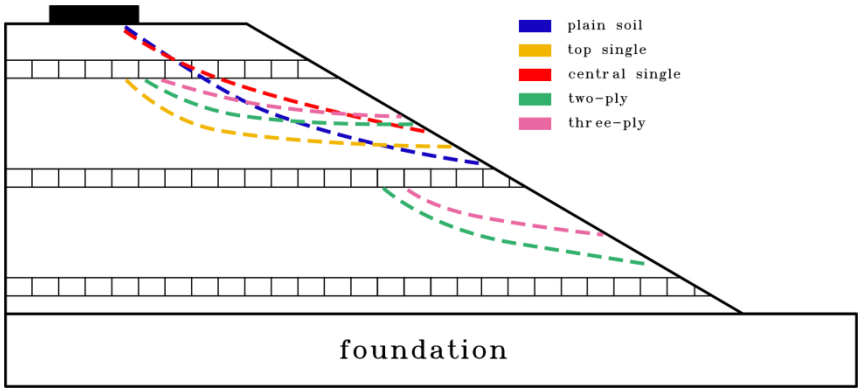

Figure 13: Embankment Spoilage Surface Morphology.

The deterioration of the sand embankment surface commences at the periphery of the loading plate and progresses towards the midpoint of the incline, but does not extend further down the slope due to the utilization of a 1:1.75 embankment side slope in the model, which represents a gentle incline. When the angle of the slope is increased, it will extend all the way to the base of the embankment. The presence of upper single layer reinforcement reduces embankment damage towards the top of the slope by increasing a portion of the rupture surface angle. This suggests that the soil mass moves away from the slope direction while also exhibiting a downward movement tendency. Additionally, the geocells experience increased friction and lateral additional soil pressure. Furthermore, the reinforcement leads to the formation of a tensile membrane effect, altering the distribution of stresses in the upper and lower layers of the reinforcement to prevent stress concentration. The lateral limiting effect of friction reduces the slope. The friction side-limiting effect reduces the deformation of the slope.

When the midpoint of the reinforcement experiences greater deformation than the slope angle, it is attributed to the distance of the reinforcement from the point of load application, which limits the effectiveness of the lattice structure.This results in lateral displacement of the soil above the reinforcement, leading to instability and damage to the embankment. Conversely, the lower section of the reinforcement layer experiences uniform loading without damage. In comparison to two layers of reinforcement, the rupture faces in the middle and lower sections are diminished in the direction moving

ISSN 2616-5767 Vol.6, Issue 12: 128-135, DOI: 10.25236/AJETS.2023.061219

away from the slope angle. This phenomenon can be attributed to the network pocket effect of the lattice chamber at the base, which constrains the displacement of the soil above, thereby preventing the embankment from collapsing at the foot of the slope and upholding the overall stability of the embankment.

4. Conclusion

This study examines the bearing capacity and deformation characteristics of geocell-reinforced windlogged sand embankments under vertical loading in five different working conditions. The initial findings and suggestions can be summarized as follows:

(1) The utilization of geocell-reinforced embankments under various operational conditions has the potential to enhance the embankment's load-bearing capacity and mitigate uneven settlement and lateral deformation. The ultimate bearing capacity can be improved by 83.3% compared to a plain sand embankment through the implementation of a three-layer reinforced condition. Additionally, the horizontal displacement of the embankment slope can be reduced by 29.17%.

(2) The reinforcement factors for geocells include the depth at which they are buried and the number of layers of reinforcement. The concentrated embankment force area is primarily located in the middle and upper sections of the embankment during the installation of geocells. This can be achieved by increasing the depth of burial within an appropriate range and adding more layers. Additionally, the use of geocells in the bottom layer of the roadbed can enhance the ultimate bearing capacity. Nevertheless, it is advantageous to minimize embankment displacement overall, and therefore, it is advisable for the actual project to incorporate two layers of reinforcing material in the upper section of the middle. It promotes the restriction of lateral deformation in the soil mass and the preservation of the overall stability of the embankment.

(3) The geocell reinforcement layer has the capability to create a composite structure with the soil, distribute the upper stress, expand the internal stress area of the embankment, and function as a friction limiter to restrict the horizontal and vertical deformation of the soil mass. This results in reduced settlement, enhanced embankment bearing capacity, and improved stability.

References

[1] Jin Shunhao. Research on reinforcement mechanism of geocell reinforced soil[D]. Northeast Forestry University, 2013.
[2] Wang Yankun. Experimental study on mechanical properties and finite element analysis of sandy soil reinforced by geocell[D]. Shihezi University, 2022. DOI:10.27332/d.cnki.gshzu.2022.000138.
[3] Indraratna B, Redana I W. Laboratory Determination of Smear Zone due to Vertical Drain Installation [J]. Geoenvironmental Engineering, 1998, 124(2). DOI:10.1061/(ASCE)1090-0241(1998) 124:2(180).
[4] Sun Zhou, Zhang Mengxi,Jiang Shengwei. Experimental study on modelling of geocell reinforced sandy embankment under bar loading[J]. Journal of Geotechnical Engineering,2015,37(S2):170-175.
[5] Wang Xuancang, Ding Longting, Fu Linjie et al. Research on the influence of geocell on roadbed stability based on centrifugal model test[J]. Highway Engineering,2019,44(05): 210-215. DOI:10. 19782/j. cnki.1674-0610.2019.05.040.
[6] Qiang Wang. Research on the performance of new geocell reinforced soil and structural optimization of reinforced high-fill embankment [D]. Wuhan University of Technology, 2020. DOI:10.27381/d. cnki. gwlgu.2020.001340.